Research article

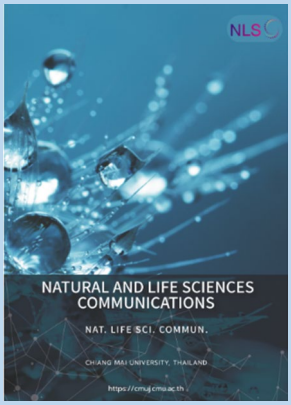

Editor:
Wipawadee Yooin,
Chiang Mai University, Thailand

Article history:
Received: June 12, 2023;
Revised: January 15, 2024;
Accepted: January 22, 2024;
Online First: January 26, 2024
https://doi.org/10.12982/NLSC.2024.002

Corresponding author:
Worrapan Poomanee,
E-mail: worrapan.p@cmu.ac.th

Development of Transethosomes Delivery System Loaded with *Bouea macrophylla* Griffith Seed Kernel Extract for Cosmeceutical Application

Phattharawadee Jaikham[1], Pimporn Leelapornpisid[1], and Worrapan Poomanee[1, 2, *]

1 Department of Pharmaceutical Sciences, Faculty of Pharmacy, Chiang Mai University, Chiang Mai 50200 Thailand.
2 Innovation Center for Holistic Health, Nutraceticals, and Cosmeceuticals, Faculty of Pharmacy, Chiang Mai University, Chiang Mai 50200 Thailand.

ABSTRACT

This research aimed to develop and optimize transethosomes loaded with *Bouea macrophylla* Griffith seed kernel extract (B-SE). Firstly, extraction procedures using solvent fractionation with various polarity: hexane, ethyl acetate and 95% (v/v) ethanol. The physicochemical properties of B-SE were investigated in terms of partition coefficient (LogP), solubility and pH-stability. To optimize the transethosomes formulation, the compositions were varied in sorts of percent cosurfactant, types of cosurfactant, extract concentration, percent total surfactant and types of particle ingredients (phospholipid or cholesterol). The significant factors influencing physical characteristics of the transethosomes were statistically identified using the 2^{5-1} fractional factorial design. Particle size, polydispersity index (PDI), percent entrapment efficiency (%EE) and ultrastructural morphology of the optimized formulation was then characterized. As a marker of B-SE, ellagic acid (EA) was identified by HPLC at a retention time of 32.506 ± 0.16 min. The LogP of B-SE was 0.17. B-SE was practically insoluble in water but freely soluble in propylene glycol and ethanol. The pH condition that stabilized the extract was pH-5. The optimized formulation, consisted of phospholipid, propylene glycol, TWEEN 20, SPAN 80 and 2.5 mg/ml of B-SE presenting particle sizes of 79.72 ± 2.42 nm, PDI of 0.26±0.02 and %EE of 83.10±0.03% along with a spherical particle shape. To conclude, the optimized transethosomes loaded with B-SE fabricated by phospholipid and propylene glycol has desirable attributes for further developing into an anti-acne cosmeceutical. Nonetheless, the bioactivities and safety profile of the transethosomes were necessary for further investigation.

Keywords: *Bouea macrophylla* Griffith, Transethosomes, Ellagic acid, Fractional factorial design, Nanocarrier

Funding: The authors are grateful for the Teaching Assistants and Research Assistants scholarship research funding provided by the Graduate School, Chiang Mai University, Thailand and the faculty of Pharmacy, Chiang Mai University, Thailand.

Citation: Jaikham, P., Leelapornpisid, P. and Poomanee, W. 2024. Development of transethosomes delivery system loaded with *Bouea macrophylla* griffith seed kernel extract for cosmeceutical application. Natural and Life Sciences Communications. 23(1): e2024002.

INTRODUCTION

Acne vulgaris is a chronic inflammation of the skin. The symptoms manifest either in the forms of open comedones or closed comedones that mostly include inflammatory reactions of the sebaceous glands in the hair follicles characterized as papules, pustules, large blisters and cysts (Zaenglein et al., 2016). The causes of acne are excessive keratinization within follicular epithelium, excess sebum production and inflammatory processes exacerbated by acne-inducing bacteria including *Cutibacterium* acnes (*C. acnes*) (formerly Propionibacterium acnes), *Staphylococcus* aureus and *Staphylococcus* epidermidis. As a result, several antibiotics have been commonly used to treat acne vulgaris. However, the antibiotics for acne treatment such as tetracyclines, minocycline, doxycycline, adapalene, erythromycin, and clindamycin have been discovered to be connected to *C. acnes* resistance continuously increases. In addition, several medicines for acne treatment produce several side effects on patients in long term use including skin sensitivity, dryness, teratogenicity and photosensitivity (Yu et al., 2016) rendering lack of patient compliance and therapeutic failure. In an effort to combat antibiotic resistance and reduce serious side effects, the use of natural extracts as alternative acne therapies has been extensively studied (Toyne et al., 2012). Moreover, at present, natural cosmetics are increasingly popular because they are considered to be safer for consumers than synthetic chemicals.

Bouea macrophylla Griffith, also known as plum mango, gandaria, and Marian plum, is a member of the Anacardiaceae family. This is a species of flowering plant native to Southeast Asia, specifically in Thailand, Malaysia, Myanmar, Indonesia, and the Philippines (Lim, 2012). A previous study of Maneechai et al., (2023) reported that *B. macrophylla* peels hydroethanolic extract demonstrated antioxidant and anti-tyrosinase properties with notable anti-inflammatory effects. Aside from the peel extract, several potential uses of ethanolic *B. macrophylla* seed extracts (B-SE) were also reported in terms of anti-acne-inducing bacteria, anti-oxidation, and effective anti-inflammatory effects to ameliorate acne inflammation due to its high contents of polyphenols (Poomanee et al., 2022). Moreover, the B-SE showed an anti-inflammatory activity by inhibiting the production of nitric oxide (NO) from lipopolysaccharides (LPS) in 264.7 RAW cells. The anti-inflammatory properties of the B-SE extracts demonstrated the dose-dependent inhibition of NO generation by BSE with no cytotoxicity to the cells in concentration range of 0.001-0.1 mg/mL (Poomanee et al., 2022). As a result, this extract constitutes a promising active ingredient for anti-acne cosmeceuticals. However, cosmetic products are frequently composed of biologically active substances that are unstable and susceptible to changes in light, oxidation, temperature and pH leading to undesired reactions, loss of efficacy or even degradation (Casanova and Santos, 2016). In addition, the use of biologically active substances in cosmetic products is limited due to the less skin penetration issues (Ansari et al., 2021). The proper delivery system of a bio-active substance is thus necessary to be invented to prevent chemical and physical degradation and deliver the substances to the target skin layer leading to better therapeutic outcome (Zaenglein et al., 2016).

Ethosomes, soft, fragile and malleable vesicles have been modified to improve drug delivery. These nanoparticles are made of phospholipids combinations and have significant concentrations of ethanol (Yu et al., 2016). Flexible ethosomes, which are ultradeformable properties of ethosomes, enhance drug dispersion through tiny pores leading to deeper skin layer penetration; as a result, they potentially enhance skin penetration of the

encapsulated drugs through the epidermal barrier (Kausar et al., 2019). In addition, the epidermal layer may fuse with the contents of the vesicles that would improve the fluidity of the lipid bilayer. The ethosomal systems are divided in three categories based on their constituents: classical ethosomes, binary ethosomes and transethosomes (Abdulbaqi et al., 2016). These systems' differences are discussed from several perspectives including entrapment efficiency, formulation, size, zeta potential, skin-permeation properties and stability. The new generation of ethosomes systems, namely, transethosomes have shown fundamental elements of classical ethosomes with an extra substance, such as surfactants or a penetration enhancer, in formulations conferring superior stability profile to classical ethosomes (Bragagni et al., 2012; Song et al., 2012; Meng et al., 2013; Ascenso et al., 2015). In this study, we were interested in transethosomes as a drug delivery system containing *B. macrophylla* seed kernel extract, which might enhance skin permeability and active ingredient stability. Also, this system has been used in a wide range of cosmetics, cosmeceuticals and pharmaceutical products due to ease of production using uncomplicated techniques (Godin and Touitou, 2003; Bhokare et al., 2016). *Pongamia pinnata* L. Pierre seed extract, incorporated in ethosomes for acne treatment, has indicated a significant increase in therapeutic responses (Ansari et al., 2021).

Therefore, this study aimed to develop and optimize a transethosome delivery system containing B-SE for cosmeceutical application. Firstly, physicochemical properties of B-SE in terms of solubility and stability were evaluated. Next, a transethosome delivery system was developed and optimized using the Design of Experiment (DOE) approach. Lastly, the formulations were characterized in terms of physical attributes.

MATERIAL AND METHODS

Materials

Phospholipid 90G (from soy lecithin) and n-octanol were obtained from Chanjao Longevity Co., Ltd., Bangkok, Thailand. Cholesterol was purchased from Loba Chemie, India. Acetonitrile and methanol in HPLC grade and absolute ethanol, hexane, ethyl acetate in AR grade were purchased from RCI Labscan limited, Thailand. Phosphoric acid (HPLC grade) was purchased from Merck, Germany. Propylene glycol, Polysorbate 20 (TWEEN 20), and Sorbitan monooleate (SPAN 80) were purchased from Namsiang, Thailand. Ellagic acid (EA) was purchased from Sigma-Aldrich, USA. Deionized water was generated by Millipore Milli-Q Advantage (Merck, Darmstadt, Germany) for used throughout the research.

Plant materials

B. macrophylla seeds, separated from the ripe fruits, were supplied by a Thai fruit plantation in Nakorn Nayok Province, Thailand. The plant materials were identified and authenticated by the Medicinal Plant Innovative Center, Faculty of Pharmacy, Chiang Mai University, herbarium code 0023323. The B. macrophylla seeds were dried using a hot air oven (Memmert UN55, Germany) at 45°C overnight and the seed coats were removed. Thereafter, they were ground into a fine powder before extraction.

Preparation of *B. macrophylla* seed kernel extract (B-SE)

B-SE was prepared according to the study of Poomanee et al. (Poomanee et al., 2022) in which the biological properties of the extract related to anti-acne potential were explored. The ground powder of *B. macrophylla* seed was firstly de-waxed using hexane maceration for 24 h using 3 cycles. Solvent

fractionation procedures were used to extract the dried *B. macrophylla* seeds using solvents with various polarity which involved sequential solvent extraction. The plant residue was then fractionated using ethyl acetate followed by 95% (v/v) ethanol in DI water. The ethanolic fraction was then filtered and evaporated using a rotary evaporator (Buchi®-461, Switzerland) to generate B-SE. Eventually, the B-SE, serving as an active ingredient, was stored in an amber glass bottle at -4°C until use.

Physicochemical properties of B-SE

Determination of EA contents of B-SE

EA contents were determined according to Dechsupa et al. (Dechsupa et al., 2019) with some modifications. The quantity of EA was investigated by HPLC (Prominence, Shimadzu, Japan). Chromatographic separation was performed using 0.01% phosphoric acid in water (A) and acetonitrile (B) as the mobile phases for gradient elution which was conducted as follows: 0 to 5 min, 95% of A; 5 to 7 min, 95 to 90% of A; 7 to 12 min, 90% of A; 12 to 14 min, 90 to 85% of A; 14 to 19 min, 85% of A; 19 to 21 min, 85 to 80% of A; 21 to 26 min, 80% of A; 26 to 30 min, 80 to 75% of A; 30 to 35 min, 75% of A, 35 to 37 min, 75 to 70% of A; 37 to 45 min, 70% of A; 45 to 50 min, 70 to 0% of A; 50 to 55 min, 0% of A, and 55 to 65 min, 95% of A. The analysis was carried out using UV wavelength of 270 nm and flowrate 0.8 mL/min. The stationary phase, namely, Inertsil ODS–3 reverse phase C–18 column (5 µm, 4.6×250 mm, GL Science Inc. USA) was conducted at 35°C. The B-SE or EA was dissolved in absolute methanol and filtered through a 0.22 µm filter before injection. In this experiment, the concentrations of EA for the standard curve were 0 to 120 µg/mL. Standard curve of EA, shown as the area under the EA curve (mAU: Y) as a function of EA concentrations, was subsequently constructed. The following equation represents X as EA concentration and Y as area under curve of EA. The EA concentration of the B-SE was then calculated and expressed as mg EA per g B-SE.

$$Y = 150492X - 550863,\ R^2 = 0.997$$

Determination of partition coefficients

Partition coefficients were determined according to Paszkowska et al. (Paszkowska et al., 2012) with some modifications using the standard shake flask method. The two-phase solvent system consisting of n-octanol and water (1:1 ratio) were mixed with the B-SE solution in an Erlenmeyer flask to produce a final concentration of 1 mg/mL. Then the flask was shaken using a funnel shaker for 12 hours at 120 rpm. After that, two phases were separated using a separation funnel and left for 4 hours, and following that, samples dissolved in both phases were obtained. Concentrations of the substance dissolved in the n-octanol phase was quantified by HPLC analysis using the aforementioned method. The ratio of the equilibrium concentrations (Ci) of a dissolved substance in a two-phase system was made of two mainly immiscible solvents known as the partition coefficient (P) (OECD, 1981) when n-octanol and water were involved as shown below.

$$P_{ow} = \frac{C_{\text{n-octanol}}}{C_{\text{water}}}$$

Hence, the partition coefficient (P) was the product of two concentrations and was expressed as a logarithm to base 10 (log P) (OECD, 1981).

Determination of solubility of B-SE

The solubility was preliminarily determined according to Alsammarraie et al., (Alsammarraie et al., 2019) described with some modifications. The solubility test was observed by bear eyes. The preliminary solubility study of B-SE involves various solvents that might be used to develop transethosomes delivery systems, such as ethanol, propylene glycol, TWEEN 20, SPAN 80 and water HPLC grade etc., Briefly, an accurate amount of the B-SE (10 mg) was added to 0.2 mL of each solvent gradually. The mixture was shaken and stepwise incorporated with 0.2 mL of the solvent until the completely dissolving the extract. The solubility define by the USP and BP classify the solubility regardless of the solvent used, just only in terms of quantification and have defined the criteria as given in Table 1 (Kovvasu, 2018).

Table 1. USP and BP solubility criteria.

Descriptive term	Part of solvent required per part of solute
Very soluble	Less than 1
Freely soluble	From 1 to 10
Soluble	From 10 to 30
Sparingly soluble	From 30 to 100
Slightly soluble	From 100 to 1000
Very slightly soluble	From 1000 to 10,000
Practically insoluble	From 10,000 and over

Stability testing of B-SE

The stability of the extract in various pH conditions (pH 2 to 9), physical appearance and chemical stability were evaluated. The 0.25 mg/mL of B-SE solution at its initial pH was also determined for stability profile in terms of physical properties such as appearance, clarity and color after accelerating condition as six cycles (4°C 24 h followed by 45°C 24 h: one cycle) of heating-cooling (HC). Chemical stability of the extract was evaluated using HPLC analysis to determine the remaining amount of extract compared with that of the initial (Bouranen, 2017; Mamah et al., 2017).

Development of transethosomes loaded with B-SE

Preparation of transethosomes loaded with B-SE

Transethosomes were prepared using the thin film hydration method. First, phospholipids (Phosphatidylcholine 90% (from soy lecithin)) or cholesterol, nonionic surfactants and B-SE were dissolved with absolute ethanol in a round-bottom flask. The next step was to evaporated the organic solvent using a rotary vacuum evaporator (Buchi-461, Switzerland) at 60°C for 15 to 20 minutes to form the thin film. The film was then rehydrated for an hour using mixtures of 5 and 10 % ethanol in DI water or 5 and 10% propylene glycol in DI water serving as co-surfactant of the system until an opaque suspension was created (Bhasin et al., 2011; Keerthi et al., 2013). Ultrasonication (VCX 600, Sonics & Materials, USA) was then performed to reduce the droplet size of the formulation using amplitude of 50% for 15 min (on 5 sec; off 5 sec).

Screening significant factors using 2^{5-1} fractional factorial design

The fractional factorial design was executed according to Li et al. (Li et al., 2022) with some modifications to screen significant factors influencing

the studied responses. Herein, the significant independent variables influencing physical characteristics of the transethosomes were statistically identified using the 2^{5-1} fractional factorial design. Five independent variables, namely, percent co-surfactant (X_1) relates to the percentage of ethanol or propylene glycol serving as a co-surfactant in formulating transethosomes, types of co-surfactant (X_2)relate to ethanol and propylene glycol in the transethosomes formulation, extract concentration (X_3) relates to the percentage of B-SE in the transethosomes formulation, percent total-surfactant (X_4) represents the percentage mixture of TWEEN 20 and SPAN 80 (1:4 ratio) and types of particle ingredient (X_5) represent cholesterol and phospholipid in the transethosomes formulation. Five independent variables were included in this screening step as shown in Table 2 presenting both actual and coded levels. In random run order, the batches consisting of 16 formulations were orthogonally created as shown in Table 3 using DESIGN EXPERT® Software (Version 13.0.0). The obtained transethosome formulation was then characterized in terms of particle size and polydispersity index (PDI) serving as dependent variables. The significance of each independent variable and interaction effect were statistically evaluated using ANOVA. In addition, interaction effects were expressed in terms of line graphs. The equation indicating the correlation between independent variables and dependent variables was also generated as a linear equation.

Table 2. 2^{5-1} Fractional factorial design, present code and values.

Independent Variable	Independent Variable Setting	
	Low (−1)	High (+1)
% Co-surfactant (X_1)	5	10
Types of co-surfactant (X_2)	Ethanol (EtOH)	Propylene glycol (PG)
% Extract (x_3)	0.1	0.25
% Total-surfactant (X_4)	4	6
Type-particle (X_5)	Cholesterol (CHO)	Phospholipid (PHO)

Characterization of the transethosomes formulation

Particle size and PDI

The diluted transethosomes using water in a ratio of 1:100 were prepared to measure the average particle size and PDI using a particle size analyzer (Malvern, England) (Cui et al., 2018).

Entrapment efficacy (%)

Entrapment efficacy was evaluated using the indirect method by ultrafiltration centrifugation determining the unentrapped substances in the system (Cui et al., 2018). Briefly, 4 mL of the optimized transethosome formulation loaded with B-SE solution, chosen as the most desirable formulation from DOE approach, was centrifuged using Amicron ®Ultra-4 (Merck, centrifugal filters ultracel®-100K) at 5000 rpm for 20 min. After that, the ultra-centrifugal filter solution with free B-SE was collected to determine the amounts of unentrapped extract. The quantities of unentrapped extract in the filtrates was analyzed using HPLC (Shimadzu, Japan) in terms of EA amount (Cui et al., 2018) and %EE was calculated using the equation below.

$$EE = \frac{D_t - D_f}{D_t} \times 100\%$$

where D_t is the total amount of EA loaded in the ethosomes and D_f is the amount of nonentrapped EA in the filtrate (Cui et al., 2018).

Ultrastructural morphology

Transmission electron microscopy (TEM) was employed to visualize the vesicular morphology and particle size. The optimized transethosomes formulation loaded with B-SE was diluted and dropped onto a copper grid, and dehydrated at room temperature. After that, the droplet was stained using 2% phosphotungstic acid solution before visualizing under TEM (Philips Tecni 20 Electron Microscope, Holland) (Cui et al., 2018).

Statistical analysis

All experiments were performed in triplicate. Data were presented as mean ± standard deviation (SD). DESIGN EXPERT® Software (Version 13.0.0) was used to evaluate the significance of independent factors involving transethosomes attributes using ANOVA and multiple regression approaches. Statistical significance was recognized as a P <0.05.

RESULTS

B. macrophylla seed kernel extract (B-SE)

From the extraction process, the obtained B-SE presents percentage yield of 5.41 ± 0.46% along with dark brown viscous liquid characteristic. This extract was employed as an active ingredient which was further determined for its EA content and preformulatory information before development of the formulation.

EA contents and partition coefficients (Log P) of the B-SE

As shown in Figure 1, the HPLC chromatograms of EA and B-SE at concentrations of 20 ppm and 2000 ppm, respectively, illustrated that EA is a marker of the B-SE at a retention time of 32.51 ± 0.16 minutes with a concentration of 8.76 ± 0.03 mg EA/g B-SE. The Log P of B-SE was 0.17 indicating partially hydrophilic manner. The equation of EA calibration curve is shown as follows; $Y = 150492X - 550863$ with R^2 of 0.997

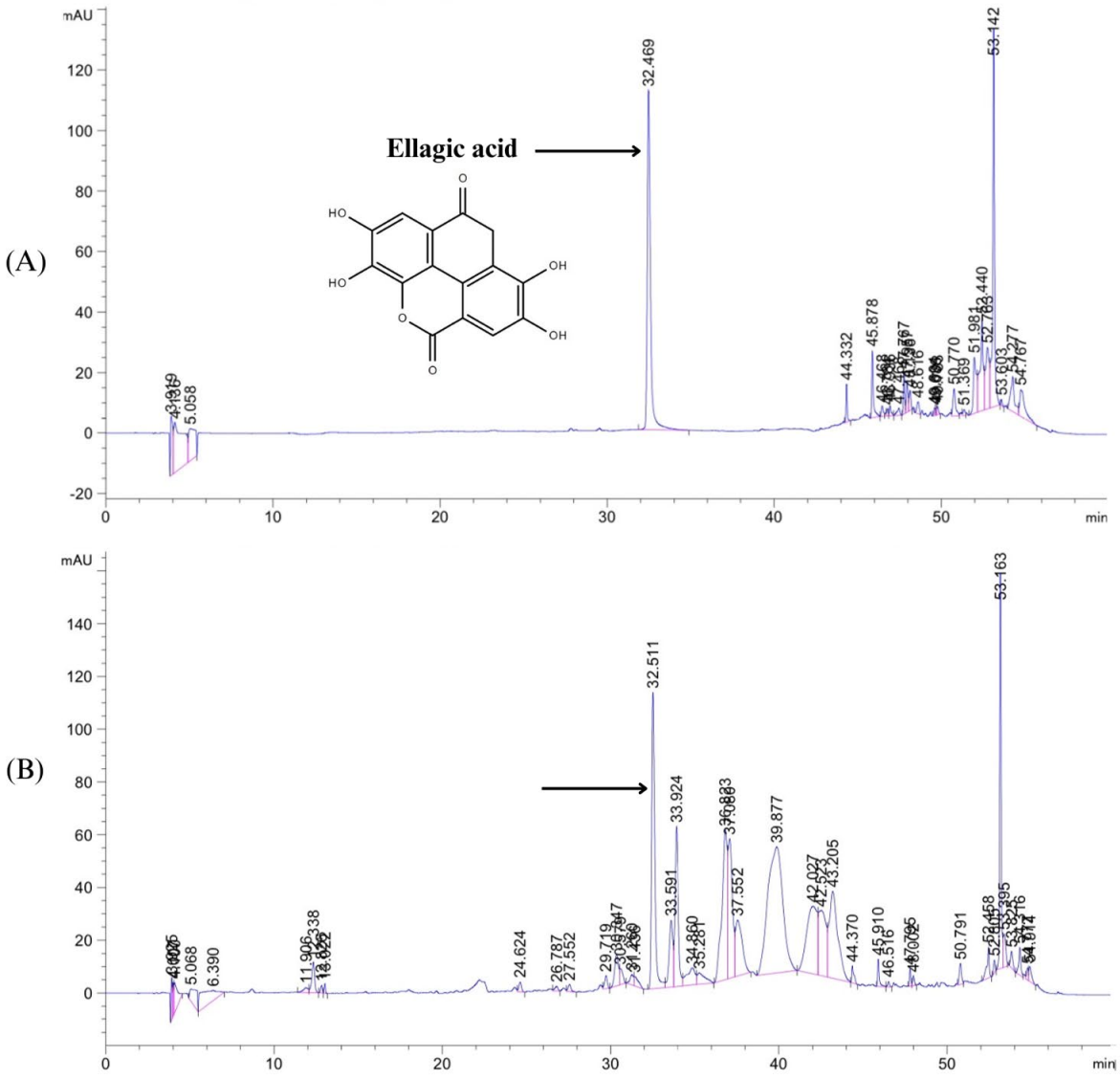

Figure 1. HPLC chromatograms of EA (EA 20 ppm) (A); B. macrophylla seeds extract (B-SE 2000 ppm) (B).

Solubility of B-SE

The results from the preliminarily solubility test indicated that, B-SE was practically insoluble in water, 5% Ethanol in DI water, 5% propylene glycol in DI water, TWEEN 20 and SPAN 80 but freely soluble in propylene glycol and absolute ethanol.

Stability of B-SE

At the initial pH of the B-SE, namely, pH 5, the B-SE solution was light yellow. After dissolving in pH of 6 to 9, the physical characteristic of the B-SE changed to a greenish-brown solution. Figure 2(A) presents the minimum %change of EA comparing between the initial and after storage at pH 5 and a maximum %change at pH 7. The concentration of EA increased rapidly at pH 6 to 7. At pH 8 to 9, EA was not detected. Figure 2(B) presents the concentration of EA (mg/mL) after storing at heating-cooling for six cycles, revealing that the concentration of EA increased to the maximum at pH 7.

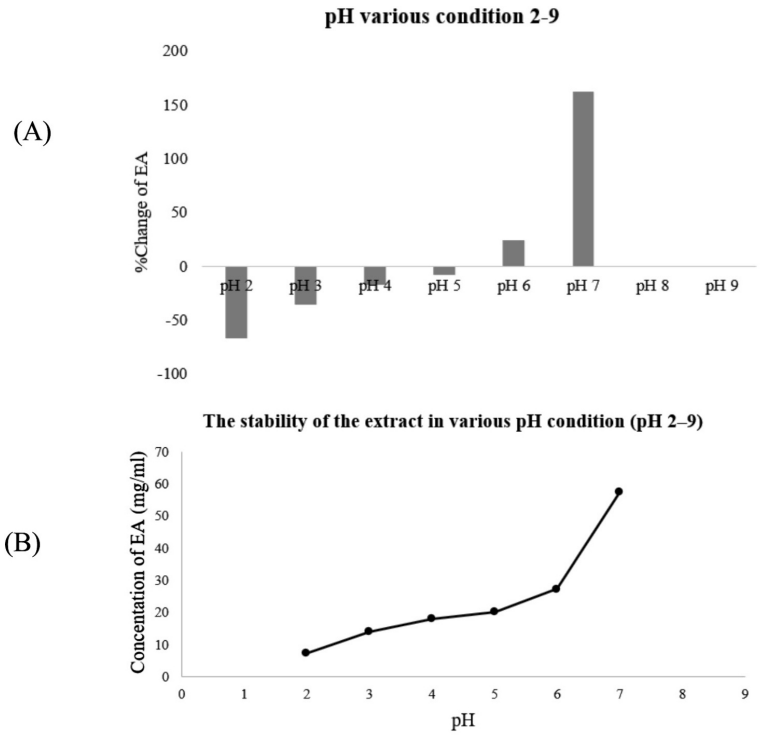

Figure 2. Percentage change of EA at various pH conditions 2-9 (A), concentration of EA at various pH 2-9 conditions and (B) after storing at heating-cooling for 6 cycles.

Significant independent variables screened by 2^{5-1} fractional factorial design

Table 3 presents the experimental matrix for 16 transethosomes formulations loaded with B-SE and the actual dependent variables. The particle size and PDI of the obtained transethosomes ranged from 74.9 to 774.8 nm, 0.254 to 0.79 and -1.9 to -9.6, respectively, suggesting that the independent variables influenced the physical attributes of transethosomes.

Table 3. Experimental matrix for transethosomes formulation loaded with B-SE and the obtained dependent variable.

Run	Variable					Response	
	X_1	X_2	X_3	X_4	X_5	Size	PDI
1	10	EtOH	0.25	6	CHO	142.40	0.79
2	10	PG	0.25	4	CHO	96.09	0.46
3	10	PG	0.25	6	PHO	82.67	0.36
4	10	EtOH	0.10	4	CHO	151.00	0.77
5	5	EtOH	0.25	6	PHO	207.00	0.46
6	5	PG	0.10	4	CHO	116.90	0.34
7	10	EtOH	0.25	4	PHO	300.20	0.66
8	10	EtOH	0.10	6	PHO	253.30	0.63
9	5	PG	0.25	4	PHO	79.72	0.26
10	5	PG	0.25	6	CHO	198.70	0.30
11	5	EtOH	0.10	6	CHO	774.80	0.78
12	10	PG	0.10	6	CHO	288.50	0.42
13	5	EtOH	0.25	4	CHO	74.90	0.25
14	5	PG	0.10	6	PHO	79.61	0.36
15	10	PG	0.10	4	PHO	74.59	0.35
16	5	EtOH	0.10	4	PHO	258.50	0.51

Note: percent co-surfactant (X_1), types of co-surfactant (X_2), extract concentration (X_3), precent total-surfactant (X_4) and types of particle ingredient (X_5)

The linear equation describing the correlation between independent variables and particle size is shown below.

$$\text{Droplet size} = 161.85 - 34.75X_2 + 17.86X_4 + 5.10X_5 - 53.05X_2X_5 - 29.16X_4X_5 \quad (1)$$

Statistical significances of the effects in both main and interaction effects on the particle size are also shown in Table 4; the main effect of types of co-surfactant (X_2) chiefly influenced the particle size, corresponding to its high coefficient in the linear equation (1). In general, a two-factor interaction was considered a confounding term with three-factor interaction in the 2^{5-1} fractional factorial design (Anderson and Whitcomb, 2017). Nonetheless, three-factor interaction is typically reported to be an insignificant term of the model. Therefore, significant two-factor interactions as X_2X_5 and X_4X_5 were included in the final model. In addition, the interaction effect between type of co-surfactant (X_2) and type-particle (X_5) strongly affected particle size. Figure 3(A) illustrates the significant interaction between the type of co-surfactant (X_2) and type-particle (X_5) concerning particle size, where other factors were 7.5% of the co-surfactant, 0.17% extract and 5% of the total surfactant; it could be interpreted that transethosomes formulated with phospholipids and propylene glycol produced a significantly smaller particle size compared with the system with cholesterol and propylene glycol. Moreover, the mixture of phospholipid and ethanol produced significantly larger particle size compared with the system of cholesterol in low surfactant concentration as shown in Figure 3(B) where other factors were 7.45 of %co-surfactant, ethanol and 0.17% of extract. In addition, 4 to 6% of total surfactant exhibited a similar size. Therefore, the setting of phospholipid, propylene glycol and 4% of total surfactant could produce the desirable transethosomes using low surfactant level.

Table 4. Analysis of variance (ANOVA) for the 25-1 fractional factorial design of the particle size variable of transethosomes loaded with B-SE.

Source	Sum of squares	Df **	Mean square	F-value	*P*-value
Model	82884.66	5	16576.93	9.85	0.0019
X_2-Type-cosurfactant	17563.41	1	17563.41	10.43	0.0103*
X_4-%Total-surfactant	4639.12	1	4639.12	2.76	0.1313
X_5-Type-particle	378.68	1	378.68	0.22	0.6466
$[X_2X_5] = X_2X_5 + X_1X_3X_4$	40938.97	1	40938.97	24.31	0.0008*
$[X_4X_5] = X_4X_5 + X_1X_2X_3$	12370.31	1	12370.31	7.35	0.024*
Residual	15153.45	9	1683.72		
Cor Total ***	98038.11	14			

Note: * statistically significant $P < 0.05$, $R^2 = 0.85$, adjusted $R^2 = 0.861$, ** df: degree of freedom *** and Cor Total: corrected total sum of square

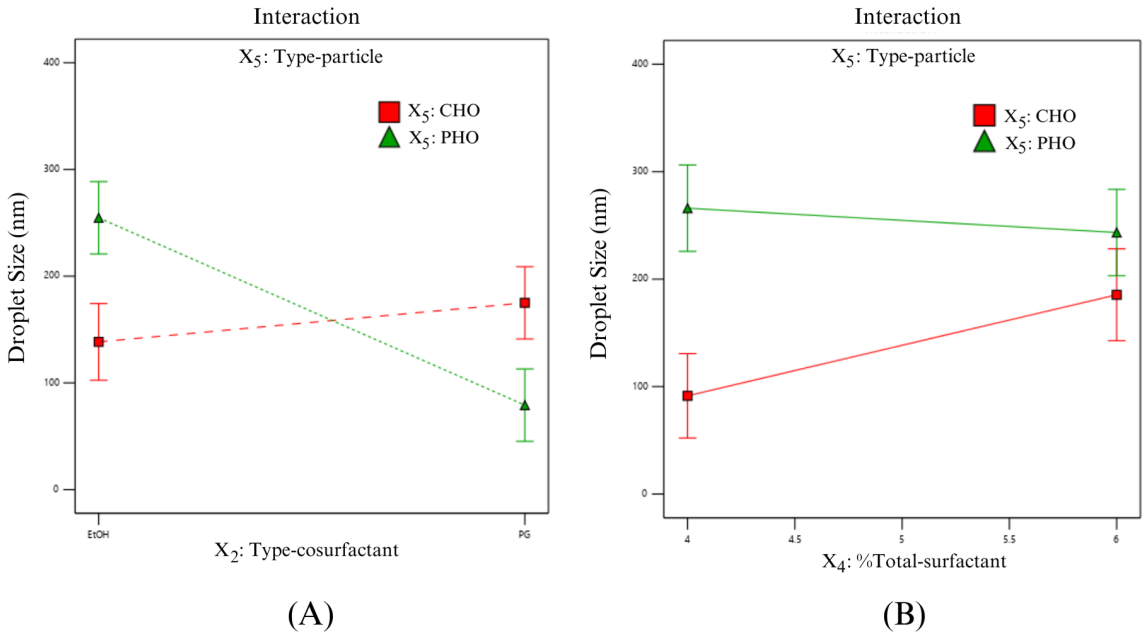

Figure 3. Line graphs presentingthe interaction between type-cosurfactant (X_2) and type-particle (X_5) on particle size (A), and the interaction between % total-surfactant (X_4) and type-particle (X_5) on particle size (B).

The linear equation (2) describing the correlation between independent variables and PDI is shown below.

$$PDI = 0.48+0.07X_1-0.13X_2-0.04X_3+0.05X_1X_3 \quad (2)$$

Statistical significances of the effect in both main and interaction effects on the PDI are shown in Table 5. The results revealed that the main effect of %co-surfactant (X_1) and types of co-surfactant (X_2) have a significant influence on the PDI. Interestingly, types of co-surfactant (X_2) mainly influenced the PDI similar to the result of droplet size. In addition, Figure 4(A) presents the interaction between %co-surfactant (X_1) and %extract (X_3), where other factors were ethanol, 5% total-surfactant and phospholipid, revealing that the transethosomes, composed of phospholipid with 5% ethanol and 0.25% extract, had a high value of PDI indicating the broadness of particle size distribution which is not a desirable property for long term storage (Shrivastava, 2018). Nevertheless, Figure 4(B) shows that phospholipid transethosomes loaded with B-SE, composed of 0.25% extract and 5% co-surfactant as propylene glycol at 5% total surfactant, exhibited a low value of PDI. This finding supported that transethosomes formulation, loaded with B-SE presenting small particle size and low PDI, should be fabricated using phospholipid combined with propylene glycol.

Table 5. Analysis of variance (ANOVA) for the 2^{5-1} fractional factorial design of PDI variable of transethosomes loaded with B-SE.

Source	Sum of squares	Df **	Mean square	F-value	*P*-value
Model	0.4055	4	0.1014	8.82	0.0019
X_1-%Co-surfactant	0.0835	1	0.0835	7.26	0.0208*
X_2- Types of co-surfactant	0.2550	1	0.2550	22.18	0.0006*
X_3-%Extract	0.0250	1	0.0250	2.17	0.1686
$[X_1X_3] = X_1X_3 + X_2X_4X_5$	0.0420	1	0.0420	3.66	0.0823
Residual	0.1265	11	0.0115		
Cor Total ***	0.5320	15			

Note: * statistically significant P <0.05, R^2 = 0.85, adjusted R^2 = 0.861, ** df: degree of freedom *** and Cor Total: corrected total sum of square

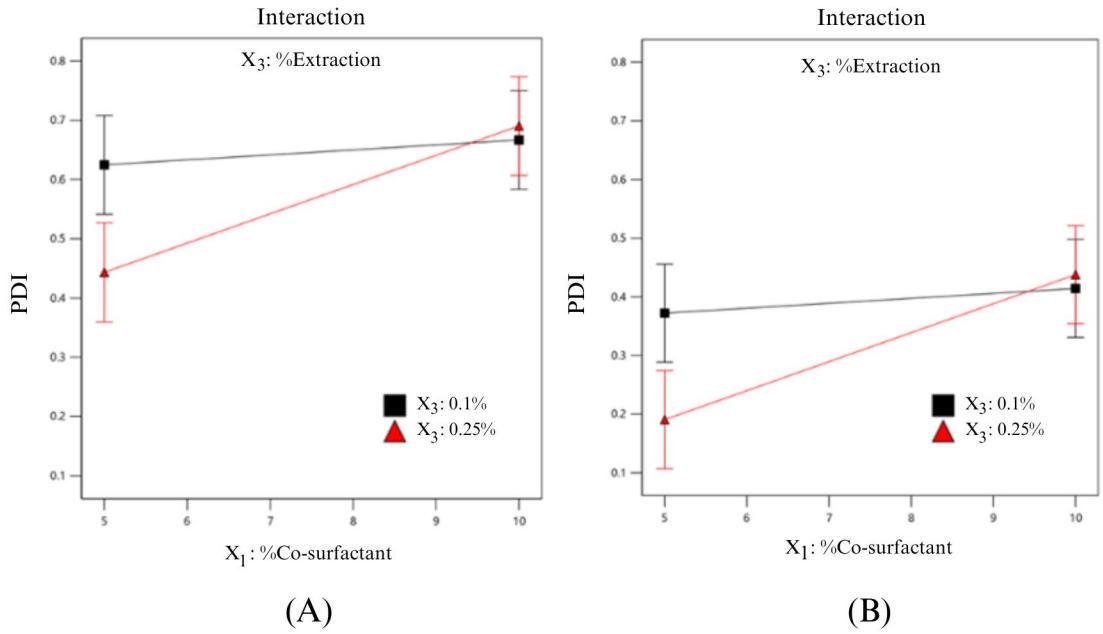

Figure 4. Line graphs presenting the interaction between %co-surfactant (X_1) and %Extract (X_3) on PDI where type-cosurfactant was ethanol (A) and the interaction between %co-surfactant (X1) and %extract (X_3) on PDI where type-cosurfactant was propylene glycol (B).

The optimized transethosomes formulation was composed of phospholipids, 5% propylene glycol, 0.25% of the B-SE, and 4% of total surfactant which was Run 9 formulation owing to its small particle size and low PDI with a good physical appearance. Therefore, the Run 9 formulation was then investigated for its characteristics in terms of entrapment efficiency (EE%) and ultrastructural morphology.

Characterization of B-SE-loaded transethosomes

The optimized transethosomes formulation loaded with B-SE as the Run 9 presented average particle sizes of 79.72 ± 2.42nm, PDI of 0.26 ± 0.02 and %EE of 83.10 ± 0.03. In addition, TEM revealed a spherical shape, double layer morphology of vesicular shell (Figure 5(A)), and fine distribution in the nano-scale similar to the result from dynamic light scattering method as shown in Figure 5(B).

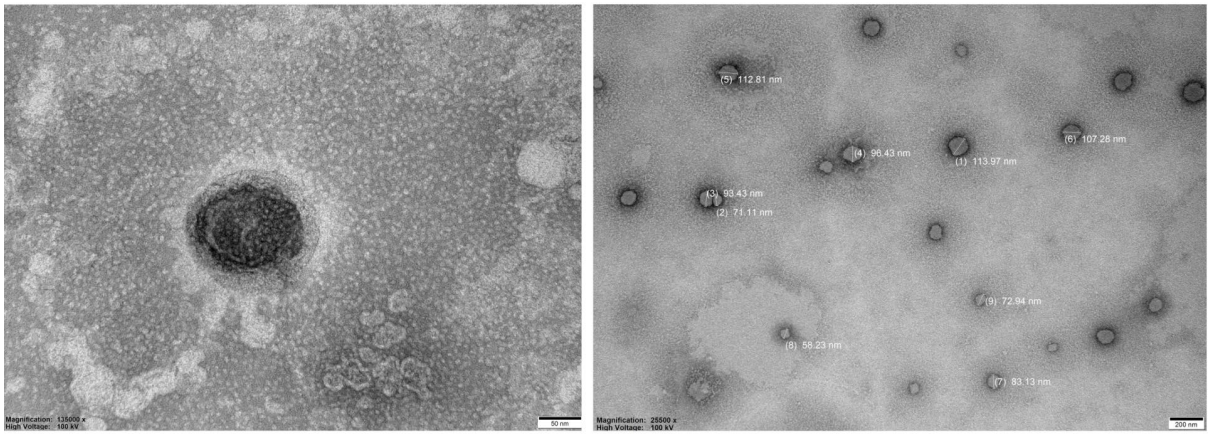

(A) (B)

Figure 5. Morphologic characterization from TEM microphotograph of Run 9 formulation spherical shape and double layer morphology (A) and distribution in the nano-range (B).

DISCUSSION

Bouea macrophylla Griffith seed extract (B-SE), of which EA has been identified as its marker, exhibit a variety of pharmacologic actions related to anti-acne potential including antibacterial, anti-oxidant and anti-inflammatory (Poomanee et al., 2022). EA is a bio-active polyphenolic compound which many plants naturally produce as a secondary metabolite. It has been proven that EA exerted several pharmacologic effects *in various in vitro* and *in vivo* experiments (Sharifi-Rad et al., 2022). In addition, EA received great interest because of its significant anti-inflammatory, anti-oxidant effects (Poomanee et al., 2022), and therapeutic potential in treating several human diseases in particular acne vulgaris (Sharifi-Rad et al., 2022). EA has the ability to prevent the growth of micro-organisms by sequestering metal ions that are essential to their metabolism and growth (Acamovic and Stewart, 1999; Aidoo et al., 1982; McDonald et al., 1996) or by inhibiting the essential functions of bacterial membrane processes that depend on pH and ionic strength, such as the activation of ion channels and proteolytic activity (Muhammed, 1997). Embedding EA on the surface membrane can alter the membrane structure by generating a hydrophobic environment around the cell and may cause protein unfolding, which will inactivate proteins (Shetty, 2004; Shetty and Labbe, 1998; Shetty and Wahlqvist, 2004). The membrane's composition may alter as a result, seriously reducing the membrane's plasticity (Tsuchiya, 2001; Tsuchiya et al., 1987). A stiff membrane weakens the cell's ability to maintain its structural integrity, impairing important transport activities and can cause the bacterial membrane to collapse (Vattem and Shetty, 2005).

Our findings in the extraction part and EA content are consistent with Poomanee et al.'s (Poomanee et al., 2022) study, which indicated that EA was found as a marker of ethanolic *B. macrophylla* seed extract. However, the concentration of EA from B-SE was significantly lower than that of the ethanolic *B. macrophylla* seed extract in the study of Poomane et al. (Poomanee et al., 2022) even though the raw material was obtained from a similar resource but in different year of harvesting. This finding could be interpreted that quality control of the plant material in terms of phytochemical content and biological activities should be necessarily executed in every batch of extraction.

The preformulatory result in terms of the B-SE stability profile indicated that pH condition at 5 could stabilized the extract well. On the contrary, at high pH, EA within the extract rapidly changed. EA is a planar lipophilic moiety with two biphenyl rings and a hydrophilic moiety with four hydroxyl groups and two lactone groups. Both donor (-OH) and acceptor (lactone) sites are presented in this specific structure for hydrogen bonding (Zuccari et al., 2020). Our result of EA stability is consistent with Bala's (2006) study in which EA was reported to have a pKa of 5.6. It became mono-deprotonated when the acidic pH was lower than 5.6 (Hasegawa et al., 2003). In contrast, EA was mainly deprotonated on the position two hydroxyl group at around neutral pH (pH 6-7). EA derivatives and native ellagitannins undergo chemical decomposition, causing the detection of a higher amount of EA compared with that stored initially. Sójka et al., (2019) reported that native ellagitannins hydrolyzed to intermediate products (sanguiin H-10 isomers, sanguiin H-2, and galloyl-HHDP-glucose isomers) at a pH 6 in aqueous solutions, with ellagic and gallic acids being the principal end products (Sójka et al., 2019). Furthermore, the basic pH is between 8 and 9, and lactone rings were opened to produce a carboxyl derivative (Bala et al., 2006), thereby, presenting loss of the compound. In addition, the Log P of B-SE was 0.17 indicating a partially hydrophilic manner. The results in the present study provided evidence that the use of B-SE in cosmeticeuticals is limited due to poor skin bioavailability associated with low solubility and limited skin permeability (Bala et al., 2006; Samineni et al., 2022; Zuccari et al., 2020). Incorporating drugs in lipid and surfactant-based nanostructures is a potential strategy to combat bioavailability (Zuccari et al., 2020).

Transethosomes represent the new generation of ethosomal systems. This ethosomal system includes a substance, such as a surfactant or a penetration enhancer, in addition to the fundamental elements of traditional ethosomes (Abdulbaqi et al., 2016). Herein, ethosomes formulation was employed owing to its flexible and elastic manner, namely, ultradeformable properties of ethosomes, enhancing medicinal dispersion through tiny pores and deep skin layer penetration. Ethosomes are flexible, soft vesicles designed for better active agent delivery because of ethosomes' distinctive structure; they can enclose and deliver cationic drugs as well as highly lipophilic molecules through the skin (Godin and Touitou, 2003). In addition, ethosomes are smaller in size compared with conventional liposomes (164.6 ± 45.6 and 182.2 ± 15.5, respectively) with comparable lipid content (30 mg of Lipoid S100), a high payload for both lipophilic and hydrophilic therapeutics and excellent physical stability during storage (Song et al., 2012). B-SE might be encapsulated in the hydrophilic core of transethosomes. In this study, transethosomes loaded with B-SE were fabricated and the significant independent variables were statistically identified using 2^{5-1} fractional factorial design. Several variables influenced the development of transethosomes and may have imparted characteristics, such as particle size and PDI of the transethosomes loaded with the drugs (Li et al., 2022). In a typical experiment or One-Factor-At-A-Time (OFAT) approach, one variable changes at a time while the others are kept at constant level producing many experiments to study only one variable. Moreover, the interaction effect which possibly had a significant impact on the responses was unable to be explored using the OFAT approach. Therefore, assessing several factors in one experimental set to identify significant independent variables and interaction terms is a great cost-effectiveness procedure. Typically, the full-factorial design for experimentation encompasses all factor combinations and offers useful insights in their interactions. Yet, even when the components at only two levels of each factor are tested, the number of experimental runs quickly rises. Thus, fractional factorial designs have been invented to serve as effective tools for precisely screening the main effects with a 2 fold lower number of experimental runs compared with the full factorial

design. In contrast to the typical experiment, a 2^{5-1} fractional factorial design potentially yields fruitful information with fewer experiments (Araújo et al., 2009). However, the interaction effect produced from fractional factorial design can't be fully trusted due to the alias or confounding issues (Anderson and Whitcomb, 2017).

Our findings implied that types of co-surfactant had the highest impact on physical attributes of the ethosomes. These compounds play a crucial role in the flexibility and elastic manner of the ethosomes system (Yu et al., 2016; Ansari et al., 2021). Most ethosomes formulations used ethanol as a co-surfactant. However, in our study, using propylene glycol together with phospholipid could produce the most designable ethosomes formulation with a double layer vesicular structure comprising the fundamental structure of this delivery system.

Several studies denoted that particle size is essential for topical delivery systems. The particle sizes which are smaller than 300 nm could penetrate their payloads in the deep skin's layers (Verma et al., 2003). Because our ethosomes formulations had sizes under 100 nm it could be assumed that these vesicles possessed the potential to deliver B-SE through the skin barrier (Yu et al., 2016). In addition, Yu et al. reported that the PDI value was less than 0.3, indicating that the size distribution of the vesicle population was relatively consistent. Entrapment efficiency is also one of the key variables to assess the system's capacity of a delivery system. Only entrapped drugs potentially penetrate to the dermal layer (Manca et al., 2013; Babaie et al., 2015; Ghanbarzadeh et al., 2015). Our optimized formulation showed a good entrapment efficiency. However, a skin permeation study should be further carried out to confirm these findings.

CONCLUSION

B-SE as an active ingredient for anti-acne cosmeceutical, showed hydrophilicity with limited skin permeation. In this study, transethosomes formulation loaded with B-SE was successfully fabricated. From the 2^{5-1} fractional factorial design, types of co-surfactant which were ethanol and propylene glycol presented the strongest influence on particle size and PDI of the system. The optimized ethosomes formulation loaded with B-SE fabricated by phospholipid and propylene glycol had desirable attributes for further development and optimization in anti-acne cosmeceutical products.

ACKNOWLEDGEMENTS

This study was supported by a research grant from Teaching Assistant and Research Assistant scholarships from the Graduate School, Chiang Mai University, and Faculty of Pharmacy, Chiang Mai University, Thailand. The authors thank the Faculty of Pharmacy, Chiang Mai University for providing all instruments and facilities.

AUTHOR CONTRIBUTIONS

Phattharawadee Jaikham carried out all of the experiments, as well as the statistical analysis and wrote original manuscript writing. Worrapan Poomanee and Pimporn Leelapornpisid designed experiments, conducted data visualization, revised the original manuscript, and supplied resources. All authors have read and approved the final manuscript.

CONFLICT OF INTEREST

The authors declare that they hold no competing interests.

REFERENCES

Abdulbaqi, I. M., Darwis, Y., Khan, N. A. K., Assi, R. A., and Khan, A. A. 2016. Ethosomal nanocarriers: The impact of constituents and formulation techniques on ethosomal properties, *in vivo* studies, and clinical trials. International Journal of Nanomedicine. 25: 2279-2304.

Acamovic, T. and Stewart, C.S. 2000. Plant phenolic compounds and gastro-intestinal microorganisms. In: Tannins in Livestock and Human Nutrition (Proceedings of an International Workshop, Adelaide, Australia, May 31-June 2 1999) Canberra, ACIAR Proceedings. No. 92 pp. 127–129.

Aidoo, K., Hendry, R., and Wood, B. 1982. Solid state fermentation. Advances in Applied Microbiology. 28: 201-237.

Alsammarraie, H. J. M., Khan, N. A. K., Mahmud, R., Bin Asmawi, M. Z., and Murugaiyah, V. A. 2019. Preformulation, stress stability studies and HPLC-UV method development and validation for 95% ethanol extract of *Moringa oleifera* Lam. leaves. Bulletin of Faculty of Pharmacy, Cairo University. 57(2): 114-126.

Anderson, M. J. and Whitcomb, P. J. 2017. DOE simplified: practical tools for effective experimentation. CRC press.

Ansari, S. A., Qadir, A., Warsi, M. H., Mujeeb, M., Aqil, M., Mir, S. R., and Sharma, S. 2021. Ethosomes-based gel formulation of karanjin for treatment of acne vulgaris: *In vitro* investigations and preclinical assessment. 3 Biotech. 11(11): 456.

Araújo, J., Vega, E., Lopes, C., Egea, M., Garcia, M., and Souto, E. B. 2009. Effect of polymer viscosity on physicochemical properties and ocular tolerance of FB-loaded PLGA nanospheres. Colloids and Surfaces B: Biointerfaces. 72(1): 48-56.

Ascenso, A., Raposo, S., Batista, C., Cardoso, P., Mendes, T., Praça, F. G., Bentley, M. V. L. B., and Simões, S. 2015. Development, characterization, and skin delivery studies of related ultradeformable vesicles: Transfersomes, ethosomes, and transethosomes. International Journal of Nanomedicine. 10: 5837.

Babaie, S., Ghanbarzadeh, S., Davaran, S., Kouhsoltani, M., and Hamishehkar, H. 2015. Nanoethosomes for dermal delivery of lidocaine. Advanced Pharmaceutical Bulletin. 5(4): 549.

Bala, I., Bhardwaj, V., Hariharan, S., and Kumar, M. R. 2006. Analytical methods for assay of ellagic acid and its solubility studies. Journal of Pharmaceutical and Biomedical Analysis. 40(1): 206-210.

Bhasin, V., Yadav, H., Markandeywar, T., and Murthy, R. 2011. Ethosomes: The novel vesicles for transdermal drug delivery. IJPI's Journal of Pharmaceutics and Cosmetology. 2(7): 68-80.

Bhokare, S. G., Dongaonkar, C. C., Lahane, S. V., Salunke, P. B., Sawale, V. S., and Thombare, M. S. 2016. Herbal novel drug delivery: A review. World Journal of Pharmacy and Pharmaceutical Sciences. 5(8): 593-611.

Bouranen, A. 2017. Determination of the stability of cosmetic formulations with incorporation of natural products (Doctoral dissertation, Instituto Politecnico de Braganca (Portugal)).

Bragagni, M., Mennini, N., Maestrelli, F., Cirri, M., and Mura, P. 2012. Comparative study of liposomes, transfersomes and ethosomes as carriers for improving topical delivery of celecoxib. Drug Delivery. 19(7): 354-361.

Casanova, F. and Santos, L. 2016. Encapsulation of cosmetic active ingredients for topical application–a review. Journal of Microencapsulation. 33(1): 1-17.

Cui, Y., Mo, Y., Zhang, Q., Tian, W., Xue, Y., Bai, J., and Du, S. 2018. Microneedle-assisted percutaneous delivery of paeoniflorin-loaded ethosomes. Molecules. 23(12): 3371.

Dechsupa, N., Kantapan, J., Tungjai, M., and Intorasoot, S. 2019. Maprang "*Bouea macrophylla* Griffith" seeds: Proximate composition, HPLC fingerprint, and antioxidation, anticancer and antimicrobial properties of ethanolic seed extracts. Heliyon. 5(7): e02052.

Ghanbarzadeh, S., Hariri, R., Kouhsoltani, M., Shokri, J., Javadzadeh, Y., and Hamishehkar, H. 2015. Enhanced stability and dermal delivery of hydroquinone using solid lipid nanoparticles. Colloids and Surfaces B: Biointerfaces. 136: 1004-1010.

Godin, B. and Touitou, E. 2003. Ethosomes: New prospects in transdermal delivery. Critical Reviews in Therapeutic Drug Carrier Systems. 20(1): 63-102.

Hasegawa, M., Terauchi, M., Kikuchi, Y., Nakao, A., Okubo, J., Yoshinaga, T., Hiratsuka, H., Kobayashi, M., and Hoshi, T. 2003. Deprotonation processes of ellagic acid in solution and solid states. Monatshefte für Chemie/Chemical Monthly. 134: 811-821.

Kausar, H., Mujeeb, M., Ahad, A., Moolakkadath, T., Aqil, M., Ahmad, A., and Akhter, M. H. 2019. Optimization of ethosomes for topical thymoquinone delivery for the treatment of skin acne. Journal of Drug Delivery Science and Technology. 49: 177-187.

Keerthi, A., Srujan Kumar, M., and Dr Subrahmanyam, K. 2013. Formulation of ethosomal gel for transdermal delivery of tramadol hydrochloride. International Journal of Innovative Pharmaceutical Sciences and Research. 1(2): 281-295.

Kovvasu, S. P. 2018. Cyclodextrins and their application in enhancing the solubility, dissolution rate and bioavailability. Innoriginal International Journal of Sciences. 5(5): 25-34.

Li, D., Martini, N., Wu, Z., Chen, S., Falconer, J. R., Locke, M., Zhang, Z., and Wen, J. 2022. Niosomal nanocarriers for enhanced dermal delivery of epigallocatechin gallate for protection against oxidative stress of the skin. Pharmaceutics. 14(4): 726.

Lim, T. K. 2012. Edible medicinal and non-medicinal plants (Vol. 1). Springer.

Mamah, B., Nisan, N., Duanyai, S., and Manok, S. 2017. Development of cosmetic product from herbals in Sripoom community in Thonburi area. Isan Journal of Pharmaceutical Sciences. 13(2): 80-89.

Manca, M. L., Manconi, M., Falchi, A. M., Castangia, I., Valenti, D., Lampis, S., and Fadda, A. M. 2013. Close-packed vesicles for diclofenac skin delivery and fibroblast targeting. Colloids and surfaces B: Biointerfaces. 111: 609-617.

Maneechai, P., Leelapornpisid, P., and Poomanee, W. 2023. Multifunctional biological activities and cytotoxic evaluation of *Bouea macrophylla* for cosmetic applications. Natural and Life Sciences Communications. 22(2): e2023030.

McDonald, M., Mila, I., and Scalbert, A. 1996. Precipitation of metal ions by plant polyphenols: Optimal conditions and origin of precipitation. Journal of Agricultural and Food Chemistry, 44(2): 599-606.

Meng, S., Chen, Z., Yang, L., Zhang, W., Liu, D., Guo, J., Guan, Y., and Li, J. 2013. Enhanced transdermal bioavailability of testosterone propionate via surfactant-modified ethosomes. International Journal of Nanomedicine. 3051-3060.

Muhammed, S. A. 1997. Antinutrient effects of plant polyphenolic compounds. University of Aberdeen (United Kingdom). ProQuest Dissertations Publishing.

OECD, P. 1981. Test Guideline 107, Decision of the council C (81) 30 final.

Paszkowska, J., Kania, B., and Wandzik, I. 2012. Evaluation of the lipophilicty of selected uridine derivatives by use of RP-TLC, shake-flask, and computational methods. Journal of Liquid Chromatography & Related Technologies. 35(9): 1202-1212.

Poomanee, W., Leelapornpisid, W., Trakoolpua, K., Salamon, I., and Leelapornpisid, P. 2022. Ameliorative effect of *Bouea macrophylla* Griffth seed extract against bacteria-induced acne inflammation: *In vitro* study. Journal of Oleo Science. 71(10): 1521-1530.

Samineni, R., Chimakurthy, J., Konidala, S., and Samineni, R. 2022. Emerging role of biopharmaceutical classification and biopharmaceutical drug disposition system in dosage form development: A systematic review. Turkish Journal of Pharmaceutical Sciences. 19(6): 706-713.

Sharifi-Rad, J., Quispe, C., Castillo, C. M. S., Caroca, R., Lazo-Vélez, M. A., Antonyak, H., Polishchuk, A., Lysiuk, R., Oliinyk, P., and De Masi, L. 2022. Ellagic acid: A review on its natural sources, chemical stability, and therapeutic potential. Oxidative Medicine and Cellular Longevity. 2022: 3848084.

Shetty, K. 2004. Role of proline-linked pentose phosphate pathway in biosynthesis of plant phenolics for functional food and environmental applications: A review. Process Biochemistry. 39(7): 789-804.

Shetty, K., and Labbe, R. G. 1998. Food-borne pathogens, health and role of dietary phytochemicals. Asia Pacific Journal of Clinical Nutrition. 7: 270-276.

Shetty, K., and Wahlqvist, M. 2004. A model for the role of the proline-linked pentose-phosphate pathway in phenolic phytochemical bio-synthesis and mechanism of action for human health and environmental applications. Asia Pacific Journal of Clinical Nutrition. 13(1): 1-24.

Shrivastava, A. 2018. Introduction to plastics engineering. William Andrew.

Sójka, M., Janowski, M., and Grzelak-Błaszczyk, K. 2019. Stability and transformations of raspberry (*Rubus idaeus* L.) ellagitannins in aqueous solutions. European Food Research and Technology. 245: 1113-1122.

Song, C. K., Balakrishnan, P., Shim, C.-K., Chung, S.-J., Chong, S., and Kim, D.-D. 2012. A novel vesicular carrier, transethosome, for enhanced skin delivery of voriconazole: characterization and *in vitro/in vivo* evaluation. Colloids and surfaces B: Biointerfaces. 92: 299-304.

Toyne, H., Webber, C., Collignon, P., Dwan, K., and Kljakovic, M. 2012. Propionibacterium acnes (*P. acnes*) resistance and antibiotic use in patients attending Australian general practice. Australasian Journal of Dermatology. 53(2): 106-111.

Tsuchiya, H. 2001. Biphasic membrane effects of capsaicin, an active component in *Capsicum* species. Journal of Ethnopharmacology. 75(2-3): 295-299.

Tsuchiya, H., Sato, M., Kameyama, Y., Takagi, N., and Namikawa, I. 1987. Effect of lidocaine on phospholipid and fatty acid composition of bacterial membranes. Letters in Applied Microbiology. 4(6): 141-144.

Vattem, D. and Shetty, K. 2005. Biological functionality of ellagic acid: A review. Journal of Food Biochemistry. 29(3): 234-266.

Verma, D. D., Verma, S., Blume, G., and Fahr, A. 2003. Particle size of liposomes influences dermal delivery of substances into skin. International Journal of Pharmaceutics. 258(1-2): 141-151.

Yu, Z., Lv, H., Han, G., and Ma, K. 2016. Ethosomes loaded with cryptotanshinone for acne treatment through topical gel formulation. PLoS One. 11(7): e0159967.

Zaenglein, A. L., Pathy, A. L., Schlosser, B. J., Alikhan, A., Baldwin, H. E., Berson, D. S., Bowe, W. P., Graber, E. M., Harper, J. C., and Kang, S. 2016. Guidelines of care for the management of acne vulgaris. Journal of the American Academy of Dermatology. 74(5): 945-973. e933.

Zuccari, G., Baldassari, S., Ailuno, G., Turrini, F., Alfei, S., and Caviglioli, G. 2020. Formulation strategies to improve oral bioavailability of ellagic acid. Applied Sciences. 10(10): 3353.

OPEN access freely available online
Natural and Life Sciences Communications
Chiang Mai University, Thailand. https://cmuj.cmu.ac.th